

The Kennicutt-Schmidt Star Formation Relation at $z \sim 2$

Desika Narayanan^{1*}†, Thomas J. Cox^{2‡}, Christopher C. Hayward¹, Lars Hernquist¹

¹Harvard-Smithsonian Center for Astrophysics, 60 Garden St., Cambridge, Ma 02138

²Observatories of the Carnegie Institution of Washington, 813 Santa Barbara St., Pasadena, Ca, 91101

MNRAS, 412, 287

ABSTRACT

Recent observations of excited CO emission lines from $z \sim 2$ disc galaxies have shed light on the $\text{SFR} \propto \rho^N$ relation at high- z via observed $\Sigma_{\text{SFR}} - \Sigma_{\text{COJ}=2-1}^\alpha$ and $\Sigma_{\text{SFR}} - \Sigma_{\text{COJ}=3-2}^\alpha$ relations. Here, we describe a novel methodology for utilising these observations of high-excitation CO to derive the underlying Schmidt ($\text{SFR} \propto \rho^N$) relationship. To do this requires an understanding of the potential effects of differential CO excitation with SFR. If the most heavily star-forming galaxies have a larger fraction of their gas in highly excited CO states than the lower SFR galaxies, then the observed molecular Kennicutt-Schmidt index, α , will be less than the underlying $\text{SFR} \propto \rho^N$ index, N . Utilising a combination of SPH models of galaxy evolution and molecular line radiative transfer, we present the first calculations of CO excitation in $z \sim 2$ disc galaxies with the aim of developing a mapping between various observed $\Sigma_{\text{SFR}} - \Sigma_{\text{CO}}^\alpha$ relationships and the underlying $\text{SFR} \propto \rho^N$ relation. We find that even in relatively luminous $z \sim 2$ discs, differential excitation does indeed exist, resulting in $\alpha < N$ for highly excited CO lines. This means that an observed (e.g.) $\Sigma_{\text{SFR}} - \Sigma_{\text{COJ}=3-2}^\alpha$ relation does not map linearly to a $\Sigma_{\text{SFR}} - \Sigma_{\text{H}_2}^\alpha$ relation. We utilise our model results to provide a mapping from α to N for the range of Schmidt indices $N = 1 - 2$. By comparing to recent observational surveys, we find that the observed $\Sigma_{\text{SFR}} - \Sigma_{\text{COJ}=2-1}^\alpha$ and $\Sigma_{\text{SFR}} - \Sigma_{\text{COJ}=3-2}^\alpha$ relations suggest that an underlying $\text{SFR} \propto \rho^{1.5}$ relation describes $z \sim 2$ disc galaxies.

Key words: galaxies: star formation–galaxies:formation–galaxies:high-redshift–galaxies:starburst–galaxies:ISM–galaxies:ISM–ISM:molecules–comology:theory

1 INTRODUCTION

Since the original works by Schmidt (1959) and Kennicutt (1998b) parameterising star formation rates (SFRs) in galaxies in terms of the scaling relation:

$$\text{SFR} \propto \rho_{\text{gas}}^N \quad (1)$$

there have been considerable efforts by both the Galactic and extragalactic star formation communities to characterise the exponent N (e.g. Kennicutt 1998a, and references therein). Constraining the Schmidt SFR relation in galaxies is desirable, both for understanding the physics of star formation on local scales, as well as for giving simulators recipes for modeling processes below typical numerical resolution scales.

Because the volume density is not observable, most observed forms of Equation 1 have been in terms of the SFR and gas sur-

face densities¹. As a result of recent pioneering high resolution millimetre-wave surveys, two trends have become apparent.

First, the SFR surface density in galaxies is well correlated with the *molecular* gas surface density, though little relation exists between the SFR and HI atomic gas (e.g. Bigiel et al. 2008; Leroy et al. 2008; ?). Second, the *global* integrated relationship between SFR and CO molecular gas surface densities in observations of local galaxies carries an exponent $N \sim 1.5$ (e.g. Sanders et al. 1991; Kennicutt 1998b; Gao & Solomon 2004a,b). A variety of theories have been proposed to explain the $N \sim 1.5$ index inferred from observations (e.g. Silk 1997; Tan 2000; Elmegreen 2002b; Krumholz & McKee 2005; Krumholz et al. 2009b), most of which rely on stars forming on a time scale proportional to the dynamical time scale.

¹ To remain consistent with typical literature nomenclature, we will refer to the volumetric form of Equation 1 as the Schmidt relation, and the surface density form as the Kennicutt-Schmidt (KS) relation. We will reserve the index, N , for the volumetric exponent, and α for the surface density exponent.

* E-mail: dnarayanan@cfa.harvard.edu

† CfA Fellow

‡ Carnegie Fellow

The recent advent of sensitive (sub)mm-wave interferometers has allowed, for the first time, observational constraints on the $\text{SFR} \propto \rho^N$ relation in “normal” star-forming (e.g. not starbursting) galaxies at high redshift via the detection of CO rotational emission lines (Bouché et al. 2007; Iono et al. 2009; Daddi et al. 2009, 2010; Bothwell et al. 2009; Genzel et al. 2010; Tacconi et al. 2010). However, owing to the fact that most mm-wave interferometers operate in the 1-3 mm wavelength regime, most detections of CO emission lines at high-redshift are of relatively excited lines (e.g. CO (J=3-2), as opposed to the ground state transition which is typically used as a tracer of H₂ molecular gas.

In principle, if the excitation of CO is relatively invariant in a given sample of galaxies, one can simply make an assumption regarding the CO (J=3-2) to (J=1-0) scaling ratio in high- z galaxies, and derive an H₂ gas mass (or surface density) with the inferred CO (J=1-0) intensity. However, if the excitation of CO in galaxies is not constant with increasing SFR, then the exponent in the $\text{SFR} \propto \text{CO}^\alpha$ relation may not naturally translate to an exponent in the $\text{SFR} \propto \rho^N$ relation. In other words, α does not always equal N when probing high excitation CO lines.

To see this, consider a sample of galaxies which are forming stars at a rate according to $\text{SFR} \propto \rho^{1.5}$. If the CO (J=1-0) line faithfully traces the H₂ gas mass, then one could expect an observed relationship $\Sigma_{\text{SFR}} \propto \Sigma_{\text{COJ=1-0}}^{1.5}$ (Krumholz & Thompson 2007; Narayanan et al. 2008c). However, if the galaxies with the highest SFR have a higher fraction of their CO gas excited into the CO J=3 state than the lowest SFR galaxies, one will observe a *flatter* relationship between SFR and $\text{L}_{\text{CO3-2}}$ than index $\alpha = 1.5$. The $\Sigma_{\text{SFR}} - \Sigma_{\text{COJ=3-2}}^\alpha$ relation will only map linearly to the $\Sigma_{\text{SFR}} - \Sigma_{\text{H}_2}^\alpha$ relation if the excitation of CO is invariant with SFR. In practice, this can only happen if the CO gas is thermalised in the observed lines (if a given excited state is in LTE).

This effect of differential molecular excitation on observed molecular SFR scaling relations has been observed in the local Universe. The SFR-CO (J=1-0) relationship has an index $\alpha \approx 1.5$, while the SFR-CO (J=3-2) relationship has a flatter index $\alpha \approx 0.9$ (Sanders et al. 1991; Yao et al. 2003; Narayanan et al. 2005; Iono et al. 2009; Bayet et al. 2009). Similarly, while the SFR-HCN (J=1-0) relationship is linear in local galaxies, the SFR-HCN (J=3-2) index is decidedly sublinear (with index $\alpha \sim 0.7$; Gao & Solomon 2004a,b; Bussmann et al. 2008; Graciá-Carpio et al. 2008; Juneau et al. 2009). Observations of individual star-forming clumps (which are massive enough to host stellar clusters) have been inconclusive regarding whether these global trends extend to smaller scales (Wu et al. 2005, 2010).

In the absence of a more direct tracer of H₂ gas than high-excitation CO, the potential effects of differential molecular excitation with SFR need to be quantified in order to derive the underlying SFR relation in high-redshift galaxies. The few multi-line constraints of excitation in high- z galaxies hints that CO may be subthermally excited even in the most luminous $z \sim 2$ systems (Weiß et al. 2007; Dannerbauer et al. 2009; Carilli et al. 2010; Harris et al. 2010). This indicates that applying a uniform mapping from (e.g.) CO (3-2) to CO (J=1-0) line intensities will indeed be problematic. In this arena, numerical models can offer guidance.

Our aim in this paper is to calculate the mapping of observed $\Sigma_{\text{SFR}} - \Sigma_{\text{CO}}^\alpha$ relations of excited lines (e.g. CO J=2-1 and CO J=3-2) to an underlying $\text{SFR} \propto \rho^N$ relation controlling the star formation. In Narayanan et al. (2009a,b, 2010) and Hayward et al. (2010), we have developed a merger-driven model for the formation of high-redshift ULIRGs which shows reasonable correspondence with observed SEDs, CO emission properties and number

counts (C. Hayward et al. in prep.). Here, we utilise the (idealised) progenitor disc galaxies of these model mergers to represent the star-forming discs at high- z typically observed in CO emission line surveys (e.g. Tacconi et al. 2010; Daddi et al. 2010). We combine these hydrodynamic simulations of disc galaxies with 3D non-LTE molecular line radiative transfer calculations in order to calculate the full statistical equilibrium excitation properties of the molecules. These methods allow us to determine the differential excitation of CO of $z \sim 2$ disc galaxies with respect to SFR, and derive a mapping of an observed molecular Kennicutt-Schmidt law ($\Sigma_{\text{SFR}} - \Sigma_{\text{CO}}^\alpha$) to a $\text{SFR} \propto \rho^N$ relationship.

2 NUMERICAL METHODS

Generally, our goal is to simulate galaxies hydrodynamically that serve as reasonable representations of the star forming galaxies at $z \sim 2$ residing on the “main sequence” of the SFR-M* relation (e.g. not starbursts; Noeske et al. 2007a,b). We first describe the hydrodynamic methods employed, and then follow with our parameter choices which ensure the physical properties of the model galaxies are comparable to those observed.

We simulate the hydrodynamic evolution of the gas phase of our model galaxies utilising the fully entropy-conserving N -body/SPH code GADGET-3 (Springel 2005). The main components of the code relevant to this study are the ISM and star formation prescriptions.

The ISM is modeled as multiphase in nature, with cold clouds embedded in a hotter, pressure-confining ISM (e.g. McKee & Ostriker 1977; Springel & Hernquist 2003). This ISM is pressurised against runaway fragmentation by supernovae which is handled via an effective equation of state (EOS). For details regarding this EOS, see Figure 4 of Springel et al. (2005). Here, we assume the stiffest equation of state ($q_{\text{EOS}} = 1$ in Springel et al. 2005). Because the global excitation of CO is to some degree dependent on the density structure of the ISM in the galaxy, we explore relaxing this assumption with test cases of $q_{\text{EOS}} = 0.75, 0.25$. We discuss the magnitude of uncertainty this parameter causes in the next section.

Star formation is controlled by a volumetric Schmidt-relation such that $\text{SFR} \propto \rho^N$. In order to explore the effects of this index on the observed SFR- L_{mol} relations, we have run simulations varying N between 1, 1.5 and 2. We choose these values as representative of the typical range of observed Kennicutt-Schmidt indices at high- z (e.g. Bouché et al. 2007; Bothwell et al. 2009; Daddi et al. 2010; Genzel et al. 2010). The normalisation is anchored such that the a volumetric Schmidt relation with index $N = 1.5$ returns a surface-density Kennicutt-Schmidt relation consistent with observations (Kennicutt 1998b). The normalisation of the $N = 1$ and 2 volumetric relations is forced to match the $N = 1$ relation at 20 times the density threshold for star formation. This normalisation was chosen such that a disc modeled after Milky Way parameters would have a global SFR of $\sim 2 M_\odot \text{yr}^{-1}$ for all three cases. As we will discuss later, we explore the effects of varying this normalisation by a factor of 2 in either direction.

It is worthwhile to consider that we force the stars to form according to a volumetric Schmidt relation, though a surface density Kennicutt-Schmidt relation is what is observable. Springel (2000) and Cox et al. (2006) have shown that a given Schmidt (volumetric) relation and Kennicutt-Schmidt (surface density) relation have the same exponent in disc simulations very similar to these, and we have confirmed this equivalence with

the simulations employed here. This similarity is not obvious. Schaye & Dalla Vecchia (2008) have shown that a linear mapping between Schmidt and Kennicutt-Schmidt SFR relations in numerical simulations is dependent on the choice of equation of state. The equation of state we employ (particularly the stiffest one, $q_{\text{EOS}} = 1$) is quite similar to Schaye & Dalla Vecchia (2008)’s “preferred” EOS which reproduces the linear mapping between the underlying Schmidt relation and observed Kennicutt-Schmidt relation. We therefore refer to the volumetric and surface density relations interchangeably².

The simulations are not cosmological. We simulate idealised discs in order to maximize spatial resolution (here, the gravitational softening length was $100 \text{ h}^{-1} \text{ pc}$ for baryons and $200 \text{ h}^{-1} \text{ pc}$ for dark matter). Because the simulations are not cosmological, we neglect potential gas replenishment from the IGM. However, we are less concerned with the temporal evolution of the model galaxy, but rather we aim to have the galaxy pass through phases during which it has physical parameters comparable to those inferred at $z \sim 2$. We thus initialise our simulations with $f_g=0.8$, and allow the disc to stabilise for some time. We then consider the snapshots in our model discs which have gas fractions between $f_g=0.4-0.2$ as motivated both by measurements of $z \sim 2$ galaxies of this baryonic mass (c.f. § 3.2; Erb et al. 2006; Daddi et al. 2009; Tacconi et al. 2010), as well as the typical steady-state gas fraction of galaxies above $M_{\text{bar}} > 10^{11}$ in cosmological simulations (e.g. Davé et al. 2010). In a cases where the gas fraction remains above $f_g > 0.2$, though the bulk of the gas is below the star formation threshold, we arbitrarily cut out snapshots below $\text{SFR} < 5M_{\odot} \text{ yr}^{-1}$ to remain consistent with the SFRs of observed galaxies at $z \sim 2$ (Daddi et al. 2010).

We model discs inside dark matter halos with Hernquist (1990) density distributions of mass $\sim 3 \times 10^{12} M_{\odot}$. The haloes are populated with discs who are constructed according to the Mo et al. (1998) formalism. These galaxies are bulgeless and have a total baryonic mass of $\sim 2 \times 10^{11} M_{\odot}$, comparable to massive *BzK* galaxies at $z \sim 2$ (e.g. Daddi et al. 2007; Tacconi et al. 2010).

To summarise the galaxy evolution modeling, the galaxy snapshots utilised in this study are “selected” according to particular criteria in order to represent massive high- z discs. In particular, the modeled galaxies have baryonic masses $M_{\text{bar}} \approx 2 \times 10^{11} M_{\odot}$ and gas fractions $f_g = 0.2 - 0.4$. When analysing the synthetic SEDs from these galaxies, the modeled *BzK* colors³ are consistent with selection as a star-forming *BzK* galaxy (e.g. Daddi et al. 2005). The result of this is a galaxy sample which lies on the high-mass end of the $z \sim 2$ SFR- M^* relation (Daddi et al. 2007), consistent with the typical galaxies observed for CO emission (e.g. Daddi et al. 2010; Genzel et al. 2010). This selection returns roughly $\sim 30-40$ galaxies each for the $N = 1, 1.5$ and 2 model types.

The simulation snapshots are analysed in post-processing with TURTLEBEACH in order to calculate their synthetic CO emission properties. TURTLEBEACH is a 3D non-LTE molecular

line radiative transfer code which considers both radiative and collisional (de)excitation in calculating the excitation conditions (Narayanan et al. 2006, 2008d) based on the Bernes (1979) method.

The process of calculating the excitation conditions in the molecular gas is as follows. First, the level populations (e.g. number of molecules at a given excitation level) are guessed at. Based on this, each molecular cloud in the galaxy emits CO line photons isotropically, with directions determined via Monte Carlo draws. These photons are absorbed by molecules in neighbouring clouds. Once the mean intensity, J_{ν} , is known across the grid, the collisional rates⁴ of CO with H_2 (based on the gas densities) are calculated, and the level populations are updated. At this point, model photons are re-emitted based on the new excitation conditions, and the whole process is repeated. This process is iterated upon until the level populations are converged.

We assume that half of the cold gas in the GADGET-3 simulations is in molecular form (as motivated by observations of local galaxies; Keres et al. 2003). By assuming that a constant fraction of the star-forming gas in the GADGET-3 simulations is molecular, we are effectively assuming that the Schmidt law we impose in the SPH simulations is a *molecular* Schmidt law, which we expect is reasonable. Within the H_2 gas, we assume the CO has a uniform Galactic abundance of $1.5 \times 10^{-4} / \text{H}_2$ (Lee et al. 1996).

The SPH simulations have resolution of $\sim 100 \text{ pc}$; as such, we do not have information regarding the state of the H_2 gas below these scales. Thus, subgrid techniques are necessary to account for the density distributions of molecular gas. We assume the H_2 gas in each cell is bound in giant molecular clouds (GMCs) with masses randomly drawn from the Galactic mass spectrum (Blitz et al. 2007), and density distributions following power-law spheres. The clouds follow a Galactic mass-radius relationship (e.g. Solomon et al. 1987; Rosolowsky 2005, 2007). Together, these parameters set the density distribution of H_2 gas in the model galaxies. Because the excitation of molecules is sensitive to the density distribution of gas in the galaxies, we explore the effect of these parameters on our final results. Observations of GMCs suggest a range of power-law indices, ranging from $n = 1$ to 2 (Andre et al. 1996; Fuller & Myers 1992; Walker et al. 1990). Similarly, the index on the GMC mass spectrum is thought to vary from $\gamma \approx -1.4$ to -2.8 (e.g. Elmegreen 2002a). Tests performed by Narayanan et al. (2008c) have shown that within these ranges, the CO excitation in galaxies similar to those presented here is not sensitive to choice of mass-spectrum index or cloud power-law index. Nominally, we employ $n = 1.5$ for the cloud power-law index and $\gamma = -1.8$. A more detailed description (including the underlying equations) regarding our subgrid methods can be found in Narayanan et al. (2008d). Finally, we have benchmarked our codes against literature standards (van Zadelhoff et al. 2002), and published the results in Narayanan et al. (2006).

3 RESULTS AND APPLICATION TO EXISTING OBSERVATIONS

3.1 Main Results

In Figure 1, we plot the model $\Sigma_{\text{SFR}} - \Sigma_{\text{CO}}^{\alpha}$ index, α , as a function of CO transition for three model disc galaxies. The disc galaxies form stars according to varying Schmidt laws, $\text{SFR} \propto \rho^N$, where

⁴ The rates come from the *Leiden Atomic and Molecular Database* (Schöier et al. 2005).

² It is conceivable that in nature these relations are not in fact equivalent. However, as this is presently unconstrainable, we are forced to operate under the assumption that the volumetric and surface-density exponents are indeed equivalent in real galaxies.

³ The synthetic colors are calculated with the dust radiative transfer code SUNRISE (Jonsson 2006; Jonsson et al. 2010). We refrain from describing the parameters for the dust modeling as reporting the results from these calculations is not the primary objective of this paper. The SUNRISE parameters utilised are identical to those in Narayanan et al. (2010), and we refer the interested reader to that paper for more details.

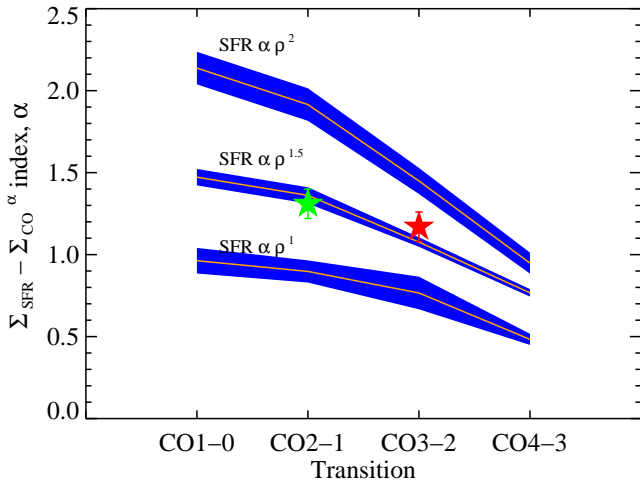


Figure 1. Predicted $\Sigma_{\text{SFR}} - \Sigma_{\text{CO}}^{\alpha}$ index, α , as a function of molecular transition for three different galaxy models. The different galaxy models vary the relation that controls their SFR such that $\text{SFR} \propto \rho^N$ where $N = 1, 1.5$ and 2 . The blue shaded region denotes the uncertainties associated with limited sample sizes. Generally, the $\Sigma_{\text{SFR}} - \Sigma_{\text{COJ=1-0}}^{\alpha}$ relation serves as a reasonable proxy for the underlying Schmidt SFR relation. With higher-lying lines, differential excitation of the molecule with SFR becomes an important effect, and the $\Sigma_{\text{SFR}} - \Sigma_{\text{CO}}^{\alpha}$ relation is flattened from the underlying $\text{SFR} \propto \rho^N$ relation. For high critical density tracers, $\alpha \neq N$. The green star shows the recent CO ($J=2-1$) data from Daddi et al. (2010), and the red star shows the CO ($J=3-2$) measurements of $z \sim 2$ galaxies by Genzel et al. (2010). This data suggests an underlying Schmidt index of $N = 1.5$.

$N = 1, 1.5$ and 2 . The top curve denotes the $N = 2$ case, middle $N = 1.5$, and bottom $N = 1$. The indices, α , are derived by fitting $\log(\text{SFR})$ versus $\log(I_{\text{CO}})$ for a random draw of 20 galaxies (corresponding to typical sample sizes in the current literature) from our parent samples of $\sim 30-40$. We do this 1000 times for each model and plot the standard deviation in the derived α -indices as the blue shaded region. We note that there is an uncertainty of $\sim 25\%$ in all mean values shown in Figure 1 based on varying initial conditions. To avoid cluttering the figure, this uncertainty is not denoted in Figure 1 itself, though will be discussed later when we provide a quantitative mapping between the Schmidt and Kennicutt-Schmidt indices. The bulk of the arguments made in this paper are summarised in this figure.

First, we see that CO ($J=1-0$) generally serves a good tracer of the H_2 molecular gas, and that the $\Sigma_{\text{SFR}} - \Sigma_{\text{COJ=1-0}}^{\alpha}$ relationship maps reasonably well from the underlying $\text{SFR}-\rho^N$ relation. This is because CO ($J=1-0$) has a relatively low critical density (Evans 1999), and most of the molecular gas emits the $J=1-0$ line. While CO ($J=1-0$) is typically optically thick *within* GMCs, owing to large velocity gradients it is optically thin on galaxy-wide scales. Thus so long as GMC properties do not vary strongly from galaxy to galaxy (as local measurements suggest; Solomon et al. 1987; Rosolowsky 2005; Blitz & Rosolowsky 2006; Blitz et al. 2007), and their mass and radius distributions are relatively narrow, then an increase in H_2 surface density will correspond to an increase in the number of GMCs, and a commensurate increase in CO ($J=1-0$) emission. For this reason, the $\Sigma_{\text{SFR}} - \Sigma_{\text{COJ=1-0}}^{\alpha}$ relation serves as a reasonably good proxy for the Schmidt relation.

The situation is different for higher excitation CO emis-

sion lines (e.g. CO $J=3-2$). Higher lying lines have relatively high critical densities. For example, the CO ($J=3-2$) line requires typical densities of $n \gtrsim 10^4 \text{cm}^{-3}$ to excite the line. Because of this, these lines are typically subthermal even in the most luminous high-redshift galaxies (e.g. Andreani et al. 2000; Papadopoulos & Ivison 2002; Greve et al. 2003; Hainline et al. 2006; Weiß et al. 2007; Dannerbauer et al. 2009; Carilli et al. 2010; Harris et al. 2010), and consequently do not trace the bulk of the molecular gas. For higher-lying CO lines, the emission line luminosity increases *superlinearly* with increasing mean gas density (owing to the combined effects of increased gas mass as well as increased excitation), and the observed $\text{SFR}-\text{L}_{\text{CO}}^{\alpha}$ index, α , will be less than the underlying Schmidt index, N (Krumholz & Thompson 2007; Narayanan et al. 2008c; Juneau et al. 2009).

Another way of saying this is that there is a differential excitation for galaxies with increasing SFR (or mean gas density, $\langle n \rangle$). The most heavily star-forming (densest) galaxies will have a higher (e.g.) CO $J=3-2$ /CO $J=1-0$ ratio than the lowest SFR galaxies. Then, because the SFR-CO ($J=1-0$) relationship traces the underlying Schmidt index, N , the observed (e.g.) $\text{SFR}-\text{CO} (3-2)^{\alpha}$ relation for higher lying lines will necessarily have a *flatter* relation than the underlying Schmidt relation. This trend will become more pronounced as one observes increasingly higher CO (or any molecular) transitions with higher critical densities. This is shown explicitly in Figure 1, where we see the $\text{SFR}-\text{L}_{\text{mol}}^{\alpha}$ index decrease as a function of increasing CO transition (or critical density) for all model galaxies. Moreover, this was shown to be an observed phenomena in the local Universe in recent surveys by Bussmann et al. (2008) and Juneau et al. (2009).

Figure 1 therefore provides a mapping between the $\Sigma_{\text{SFR}} - \Sigma_{\text{CO}}^{\alpha}$ relation for observed high-lying CO transitions and the underlying Schmidt relation. For the purposes of direct application to current high- z data, in Figure 2, we turn Figure 1 into an actual mapping between the $\Sigma_{\text{SFR}} - \Sigma_{\text{CO}}^{\alpha}$ index, α , and the volumetric Schmidt index, N . In particular, we focus on the CO ($J=3-2$) transition as it is a relatively commonly observed line at $z \sim 2$. The solid line is the mean from Figure 1 (e.g. the mean after randomly drawing 20 galaxies of our parent sample 1000 times). The blue shaded region denotes a 25% range of uncertainty. The uncertainty is determined by characterising the dependence of α on the input parameters. In particular, within the confines of our “selection criteria”, the input parameters which have the strongest effect on α are the equation of state and the Schmidt law normalisation (owing to their changing the gas density distribution and the level of thermalisation of the gas). We find the maximum variance in α with these parameters is less than 25%.

We can utilise a combination of recent observations of high- z star-forming systems and the information in Figures 2 and 1 to infer the Schmidt relation at high- z . Recent investigations by Daddi et al. (2010), Tacconi et al. (2010) and Genzel et al. (2010) have investigated the $\Sigma_{\text{SFR}} - \Sigma_{\text{CO}}^{\alpha}$ relation in “normal” star-forming systems at $z=1-2$ which lie on the main sequence of the $\text{SFR}-M^*$ relation. Daddi et al. (2010) find a $\Sigma_{\text{SFR}} - \Sigma_{\text{COJ=2-1}}^{\alpha}$ index of $\alpha \approx 1.31$. Similarly, Genzel et al. (2010) find a $\Sigma_{\text{SFR}} - \Sigma_{\text{COJ=3-2}}^{\alpha}$ index for their data set of $\alpha \approx 1.17$. Comparing this to Figure 1, we see that these values correspond to an underlying Schmidt index of $N = 1.5$.

Figures 1 and 2 therefore provide evidence that an Schmidt index $N \approx 1.5$ holds for high-redshift galaxies. It is important to note, however, that there is an uncertainty of $\sim 25\%$ in these models. Observations of numerous CO transitions will help to nar-

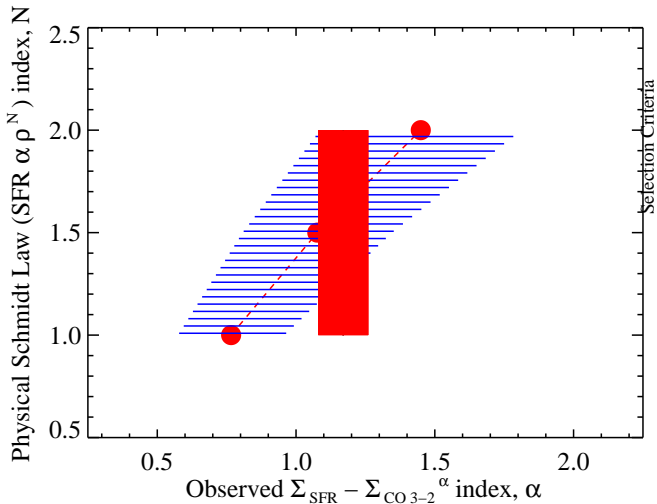


Figure 2. The relationship between the $\text{SFR} \propto \rho^N$ index, N , and the observed $\Sigma_{\text{SFR}} - \Sigma_{\text{CO}J=3-2}^\alpha$ index, α . The red dashed line represents the mean result, and the blue shaded region denotes a 25% uncertainty (see text for details). The red solid region represents the best fit to available CO ($J=3-2$) data from $z \sim 2$ discs (Genzel et al. 2010), and the thickness represents the associated uncertainty. The intersection of the observed $\Sigma_{\text{SFR}} - \Sigma_{\text{CO}J=3-2}^\alpha$ index, α and the model results suggests that a Schmidt index of $N \approx 1.5$ may appropriately describe $z \sim 2$ disc galaxies.

row the uncertainty in the derived $\text{SFR} \propto \rho^N$ relation by providing additional constraints in the $N - \alpha$ space probed in Figure 2. In Table 1, we provide the mapping between Schmidt indices, N and molecular Kennicutt-Schmidt indices, α for four CO transitions. These numbers provide enough information to create $N - \alpha$ plots similar to Figure 2 for transitions other than CO ($J=3-2$), and test the concept that a Schmidt index of $N \approx 1.5$ describes star formation in high- z galaxies.

3.2 Uncertainties and Dependence on Model Physical Parameters

In Figure 3, we show the simulated $\Sigma_{\text{SFR}} - \Sigma_{\text{CO}J=1-0}^\alpha$ plot for our model with a Schmidt index of $N = 1.5$, and denote the galaxies which fall within our selection criteria. The trends in Figure 1 can depend on how large of a dynamic range the mock observations span.

The trends in Figure 1 depend on the degree of differential excitation, which depends on the dynamic range of SFR surface densities (or gas surface densities) observed. For example, consider the case where observations only probe a limited range of extremely high SFR galaxies (here, we take this to mean galaxies with gas fraction $0.4 < f_g < 0.8$). In the high gas fraction/high SFR regime, the excitation conditions vary extremely rapidly. The most gas-rich, densest systems have much of their gas thermalised, whereas lower gas fraction galaxies in this range ($f_g \approx 0.4 - 0.6$) begin to contain subthermal gas. While it may seem counterintuitive that some high gas-fraction galaxies may not be fully thermalised in higher CO lines, it is important to remember that the simulations (as do observations) consider *global* emission, from both low and high-density regimes. Subthermal CO level populations have been noted both in observations of local galaxies (Narayanan et al. 2005, 2008a; Iono et al. 2009), as well as in observations of even the densest, most heavily star-

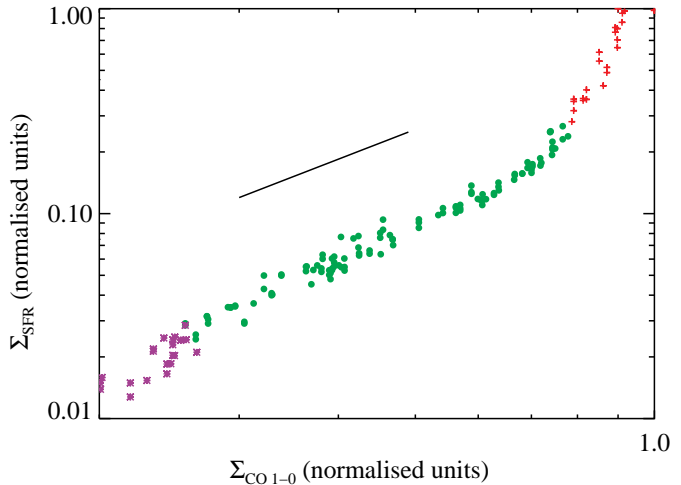


Figure 3. The model $\Sigma_{\text{SFR}} - \Sigma_{\text{CO}J=1-0}^\alpha$ relation for our model with underlying Schmidt index $N = 1.5$. The solid line shows a slope of $N = 1.5$. The ordinate and abscissa are in normalised units. The green circles show the galaxies that satisfy our “selection” criteria cuts. Including extremely gas-rich (red plus signs) or gas-poor systems (where most of the gas is below the star formation threshold; purple crosses) may cause the observed KS indices to deviate from those in Figure 1

forming submillimetre-galaxies at high-redshift (Carilli et al. 2010; Harris et al. 2010). The rapidly dropping CO excitation (from the higher J states to the ground states) at the highest SFRs causes the observed molecular KS relation to steepen from the underlying Schmidt relation. In the fiducial case of the $N = 1.5$ galaxy, the observed $\Sigma_{\text{SFR}} - \Sigma_{\text{CO}J=1-0}^\alpha$ index can range from ~ 1.5 to ~ 2.7 as we consider increasing numbers of galaxies with gas fractions beyond $f_g > 0.4$ in the fits.

The molecular KS relation at the other end of the spectrum, in gas-poor galaxies, is less clear. On one hand, we can expect that it would steepen owing to the bulk of the gas in the galaxy being below the SF threshold (see, e.g. Bigiel et al. 2008). However, our models don’t consider the possible destruction of molecular gas in low density environments (e.g. Krumholz et al. 2009a). At low densities, the neutral ISM is a mixture of HI and H_2 . This is not captured by our models as we are forced by lack of resolution to consider the H_2 as a fixed fraction of the neutral ISM mass. In reality, if the H_2 and/or CO mass also drops at low densities, the observed KS relation may not become as steep as Figure 3 would suggest.

The trends predicted in Figure 1 are relatively robust within the physical parameter range chosen for the bulk of this paper ($0.2 < f_g < 0.4$, with a typical dynamic range in SFR of order ~ 10). As was just shown, large deviations from galaxies of this sort may change the observed mapping from a Schmidt relation to a KS relation. That said, our assumed range of gas fractions may accurately represent real $z \sim 2$ galaxies. For example, cosmological hydrodynamical simulations suggest that most galaxies with baryonic masses $>$ a few $\times 10^{11} M_\odot$ (comparable both to those modeled, as well as those observed) have steady-state gas fractions of order $\sim 0.2-0.4$ (e.g. Davé et al. 2010). Recent observations appear to come to a similar conclusion. For example, CO measurements of BzK galaxies by Daddi et al. (2009) suggest that the expected gas fraction for galaxies of the baryonic mass modeled here are $f_g \sim 0.4$. Similarly, by inversion of the Kennicutt-Schmidt rela-

tion, Erb et al. (2006) suggest gas fractions of massive star-forming galaxies of order $f_g \approx 0.2 - 0.4$. Finally, a large CO survey by Tacconi et al. (2010) suggest that the distribution of gas fractions of normal, star-forming galaxies in this mass range between $z=1-3$ is relatively sharply peaked at $f_g = 0.3 - 0.4$ with only rarer excursions outside of this range.

It is additionally worth discussing the potential effects of our ISM assumptions on our modeled results. As was discussed in § 2, the hydrodynamic galaxy evolution calculations cannot resolve giant molecular clouds, the primary origin site of CO emission lines. Because of this, we are forced to utilise a subgrid prescription for including GMCs in the radiative transfer calculations. In the absence of any observational constraints of the nature of the structure of the molecular ISM at high- z , we assume that clouds exist as bound spheres, following a Galactic mass-spectrum and Galactic mass-radius relation with a power-law density gradient (see Narayanan et al. 2008b, for the actual underlying algorithms).

Our model results are dependent on this assumption. As was shown in Krumholz & Thompson (2007) and Narayanan et al. (2008c), the degree of differential excitation in galaxies comes from the shape of the high-density tail of the molecular gas density distribution. While determining the exact dependence of the molecular excitation on the density distribution of molecular gas is worthy of an independent study, previous model results suggest that a range of reasonable assumptions result in similar differential excitation patterns. For example, Krumholz & Thompson (2007) assumed a log-normal density distribution in their model galaxies, whereas Narayanan et al. (2008c) utilised a numerical model derived from the aforementioned cloud mass spectrum, mass-radius relation, and power-law density distribution within clouds. Both studies found a similar degree of differential excitation in local galaxies (see, e.g., the similar predictions for the SFR-HCN 3-2 relation in local galaxies between the two models in Figure 2 of Bussmann et al. 2008). In this sense, our model assumptions for the structure of the molecular ISM appears reasonable, at least in the context of local galaxies⁵. In a similar vein, we note that the assumed equation of state in our models can affect the density distribution via pressurisation of the ISM. As noted in § 3.1, within the range of our modeled EOSs ($q_{\text{EOS}} = 0.25 - 1$, see Springel 2005, and § 2 for more details), we find $< 25\%$ difference in the modeled molecular KS indices.

It is conceivable, however, that the molecular gas in high-redshift galaxies is different in its structure than clouds in the Galaxy. For example, observations of local ULIRGs show that in high gravitational potentials, tides may cause the molecular ISM to exist in a smooth structure with a large volume-filling factor, rather than in bound clouds (Downes & Solomon 1998). It is not entirely clear, in these starburst galaxies, whether the density distribution is similar in shape to those in normal discs (e.g. with a high-density tail), or whether they have a substantially different gas density distribution. Resolved maps of GMCs in local ULIRGs with ALMA will help to answer this question.

Finally, we note that galaxies at high- z may have a larger fraction of their gas in a dense phase than local galaxies. This is explicitly accounted for in our modeling. As described in Narayanan et al. (2008b), clouds are randomly drawn from the mass spectrum to fill

cells of a given mass until the mass-budget is used. When the density in a particular region is high (as informed by the hydrodynamic models), more high-mass clouds will statistically be drawn, thus increasing the dense gas fraction.

It is important to note, however, that the effects of radiative transfer on scales below our cell-sizes are only marginally accounted for in these models. When a photon is emitted, it sees a column density drawn randomly from the distribution of columns seen in the cell (Narayanan et al. 2008b), and deposits some intensity. However, because the velocity distribution is not modeled on sub-grid scales, this is a limiting assumption. Some of this radiation may actually emerge from the cell owing to large velocity gradients within a cell which may keep photons from being trapped. Efforts are underway to explicitly account for this effect, though it is a task well outside the scope of this study.

4 DISCUSSION

The principle result of this study is that, due to subthermal excitation in high-lying CO lines in high- z galaxies, observed $\Sigma_{\text{SFR}} - \Sigma_{\text{CO}}^\alpha$ relations do not necessarily map linearly to $\Sigma_{\text{SFR}} - \Sigma_{\text{H}_2}^\alpha$ relations. This is part of a broader theoretical framework first developed by Krumholz & Thompson (2007) and Narayanan et al. (2008c) which posits that the underlying density distribution of galaxies is crucial in mapping the underlying Schmidt relation to observed molecular Kennicutt-Schmidt relations. In this paper, we have expanded upon these studies by exploring the relationship between Schmidt and Kennicutt-Schmidt indices in models which aim to serve as reasonable representations of the $z \sim 2$ star-forming disc galaxies being uncovered in sensitive optical/NIR observations (e.g. Daddi et al. 2005; Förster Schreiber et al. 2009). Indeed, the models studied here have been shown in previous publications to satisfy the star-forming *BzK* colour-selection criteria (Narayanan et al. 2009b), as well as serve as reasonable progenitors for luminous, merger-driven $z \sim 2$ submillimetre and 24 μm -selected galaxies (Hayward et al. 2010; Narayanan et al. 2010). We have additionally explored the dependence of the observed molecular Kennicutt-Schmidt index on varying underlying Schmidt relations. Our models, combined with the general theoretical framework of Krumholz & Thompson (2007) and Narayanan et al. (2008c) suggest that observed $z \sim 2$ discs are subject to differential CO excitation with respect to SFR, and that the observed $\Sigma_{\text{SFR}} - \Sigma_{\text{COJ=2-1}}^\alpha$ and $\Sigma_{\text{SFR}} - \Sigma_{\text{COJ=3-2}}^\alpha$ relations may map to an underlying Schmidt index of $N = 1.5$ controlling the SFR.

An important verifying aspect to these models is that they are able to explain the multitude of observed SFR- L_{mol} relations in the local Universe. For example, a linear relationship has been observed between SFR and HCN ($J=1-0$) in local galaxies, a trend which has often been interpreted as evidence that a linear *dense gas* Schmidt relation controlled the SFR. Our models suggest the linear SFR-HCN ($J=1-0$) relation is in reality a combined effect of an underlying SFR $\propto \rho^N$ index of $N = 1.5$ and differential excitation in HCN (Krumholz & Thompson 2007; Narayanan et al. 2008c). This view has been observationally confirmed by Bussmann et al. (2008), who showed that local galaxies exhibit an *sublinear* SFR-HCN ($J=3-2$) relation, and thus follow the trend of decreasing SFR-HCN $^\alpha$ index with increasing transition number characteristic of these models (e.g. Figure 1; see also Figure 7 of Narayanan et al. 2008c). Similarly, this model satisfies the multi-line constraints of local CO observations. The SFR-CO ($J=1-0$) relation in local galax-

⁵ It is additionally worth noting that Narayanan et al. (2008c) varied the range of indices of the Galactic mass-spectrum and power-law density gradients within the range of observational constraints, and found little difference in the final differential excitation in their modeled local galaxies.

Table 1. This Table provides the mapping between observed Kennicutt-Schmidt molecular surface-density indices, α , and underlying volumetric Schmidt indices, N . We provide the mapping for CO transitions J=1-0 through J=4-3. The numbers contained here constitute the information necessary to re-create a plot like Figure 2 for any of the four modeled CO transitions and will aid interpretation of future observations of varying molecular transitions. The “errors” denote a 25% uncertainty level which encompasses variations in the final solution upon changing initial conditions in our simulation (primarily the equation of state and normalisation of the SFR relation).

Schmidt Index N	SFR-CO (J=1-0) $^\alpha$	SFR-CO (J=2-1) $^\alpha$	SFR-CO (J=3-2) $^\alpha$	SFR-CO (J=4-3) $^\alpha$
1	0.96±0.24	0.89±0.22	0.76±0.19	0.49±0.12
1.5	1.47 ±0.37	1.36±0.34	1.08±0.27	0.77±0.19
2	2.13 ±0.53	1.95±0.48	1.45±0.36	0.95±0.24

ies appears to have an index ranging from $\sim 1.3 - 1.5$. At higher-lying transitions (e.g. CO J=3-2), the index drops to ~ 0.9 , in accordance with theoretical predictions (Iono et al. 2009). We note that at lower bolometric luminosities, even the SFR-CO (J=1-0) relation may be subject to differential excitation and serve as a relatively poor tracer of the underlying Schmidt relation.

Finally, with an eye toward ALMA, we comment on the role of spatial resolution in observational determinations of the KS relation at high- z . The exact mapping between the observed $\Sigma_{\text{SFR}} - \Sigma_{\text{CO}}^\alpha$ index, α , and the $\text{SFR} \propto \rho^N$ index, N , depends on the level of thermalisation of the gas within the beam. It is dependent (to first order) on the mean gas density. Higher resolution observations which probe just the nucleus of the galaxy will probe higher mean densities, and allow even higher-lying CO emission lines to directly trace the underlying Schmidt SFR relation. Indeed, some very tentative observational evidence for this trend in local galaxies has been shown by Narayanan et al. (2008a). The trends shown in Figures 1 and 2 are for the central 6 kpc of the galaxy, comparable to the typical resolution of current interferometric observations of $z \sim 2$ galaxies (e.g. Tacconi et al. 2010). Our models suggest that observations of the central ~ 2 kpc will probe sufficiently dense gas that the observed $\Sigma_{\text{SFR}} - \Sigma_{\text{COJ=3-2}}^\alpha$ index, α , will trace the underlying $\text{SFR} \propto \rho^N$ index, N .

5 SUMMARY

Current facilities demand that observations of the molecular Kennicutt-Schmidt relation at $z \sim 2$ probe highly excited CO lines (e.g. CO J=3-2). However it is not clear how exactly to map observed $\Sigma_{\text{SFR}} - \Sigma_{\text{COJ=3-2}}^\alpha$ relations to underlying $\text{SFR} \propto \rho^N$ relations: differential excitation of CO with SFR may make interpretation difficult.

In order to aid in the interpretation of observed molecular Kennicutt-Schmidt relations, we have calculated the first models of CO excitation for star-forming disc galaxies at $z \sim 2$. Our main results are:

(i) Due to differential excitation of CO with SFR in $z \sim 2$ disc galaxies, global observations of a (e.g.) $\Sigma_{\text{SFR}} - \Sigma_{\text{COJ=3-2}}^\alpha$ relation will result in a *flatter* index, α , than the underlying Schmidt ($\text{SFR} \propto \rho^N$) index, N . This trend exists for all lines above CO (J=1-0), though the disparity between α and N grows with increasingly high CO transitions owing to increasing critical densities in the line.

(ii) We present a mapping from observed $\Sigma_{\text{SFR}} - \Sigma_{\text{CO}}^\alpha$ indices, α , to underlying Schmidt indices, N for global observations of $z \sim 2$ discs. Combining these model results with the observed (nearly) linear relationship between Σ_{SFR} and $\Sigma_{\text{COJ=3-2}}^\alpha$ suggests that a relation $\text{SFR} \propto \rho^{1.5}$ may control the SFR in $z \sim 2$ galaxies.

ACKNOWLEDGEMENTS

We thank Shane Bussmann, Neal Evans, Reinhard Genzel, Patrik Jonsson, Dusan Keres, Mark Krumholz, Charlie Lada, Kai Noeske, Alice Shapley, Amiel Sternberg and Linda Tacconi for enjoyable conversations as the ideas for this study were developed. The simulations in this paper were run on the Odyssey cluster, supported by the Harvard FAS Research Computing Group.

References

- Andre, P., Ward-Thompson, D., & Motte, F. 1996, A&A, 314, 625
 Andreani, P., Cimatti, A., Loinard, L., & Röttgering, H. 2000, A&A, 354, L1
 Bayet, E., Gerin, M., Phillips, T. G., & Contursi, A. 2009, MNRAS, 399, 264
 Bernes, C. 1979, A&A, 73, 67
 Bigiel, F., Leroy, A., Walter, F., Brinks, E., de Blok, W. J. G., Madore, B., & Thornley, M. D. 2008, AJ, 136, 2846
 Blitz, L., Fukui, Y., Kawamura, A., Leroy, A., Mizuno, N., & Rosolowsky, E. 2007, in Protostars and Planets V, ed. B. Reipurth, D. Jewitt, & K. Keil, 81–96
 Blitz, L. & Rosolowsky, E. 2006, ApJ, 650, 933
 Bothwell, M. S. et al. 2009, MNRAS in press: ArXiv/0912.1598
 Bouché, N. et al. 2007, ApJ, 671, 303
 Bussmann, R. S., Narayanan, D., Shirley, Y. L., Juneau, S., Wu, J., Solomon, P. M., Vanden Bout, P. A., Moustakas, J., & Walker, C. K. 2008, ApJ, 681, L73
 Carilli, C. L. et al. 2010, ApJ Submitted: ArXiv/1002.3838
 Cox, T. J., Jonsson, P., Primack, J. R., & Somerville, R. S. 2006, MNRAS, 373, 1013
 Daddi, E., Elbaz, D., Walter, F., Bournaud, F., Salmi, F., Carilli, C., Dannerbauer, H., Dickinson, M., Monaco, P., & Riechers, D. 2010, ArXiv/1003.3889
 Daddi, E. et al. 2005, ApJ, 631, L13
 —. 2007, ApJ, 670, 156
 —. 2009, ArXiv/0911.2776
 Dannerbauer, H., Daddi, E., Riechers, D. A., Walter, F., Carilli, C. L., Dickinson, M., Elbaz, D., & Morrison, G. E. 2009, ApJ, 698, L178
 Davé, R., Finlator, K., Oppenheimer, B. D., Fardal, M., Katz, N., Kereš, D., & Weinberg, D. H. 2010, MNRAS, 404, 1355
 Downes, D. & Solomon, P. M. 1998, ApJ, 507, 615
 Elmegreen, B. G. 2002a, ApJ, 564, 773
 —. 2002b, ApJ, 577, 206
 Erb, D. K., Steidel, C. C., Shapley, A. E., Pettini, M., Reddy, N. A., & Adelberger, K. L. 2006, ApJ, 647, 128
 Evans, II, N. J. 1999, ARA&A, 37, 311
 Förster Schreiber, N. M. et al. 2009, ApJ, 706, 1364

- Fuller, G. A. & Myers, P. C. 1992, *ApJ*, 384, 523
- Gao, Y. & Solomon, P. M. 2004a, *ApJS*, 152, 63
- . 2004b, *ApJ*, 606, 271
- Genzel, R. et al. 2010, *MNRAS* accepted; arXiv/1003.5180
- Graciá-Carpio, J., García-Burillo, S., Planesas, P., Fuente, A., & Usero, A. 2008, *A&A*, 479, 703
- Greve, T. R., Ivison, R. J., & Papadopoulos, P. P. 2003, *ApJ*, 599, 839
- Hainline, L. J., Blain, A. W., Greve, T. R., Chapman, S. C., Smail, I., & Ivison, R. J. 2006, *ApJ*, 650, 614
- Harris, A. I., Baker, A. J., Zonak, S. G., Sharon, C. E., Genzel, R., Rauch, K., Watts, G., & Creager, R. 2010, *ArXiv e-prints*
- Hayward, C. C., Narayanan, D., Jonsson, P., Cox, T. J., Kereš, D., Hopkins, P. F., & Hernquist, L. 2010, *Conference Proceedings for UP2010: Have Observations Revealed a Variable Upper End of the Initial Mass Function?* Treyer, Lee, Seibert, Wyder, Neil eds. arXiv/1008.4584
- Hernquist, L. 1990, *ApJ*, 356, 359
- Iono, D., Wilson, C. D., Yun, M. S., Baker, A. J., Petitpas, G. R., Peck, A. B., Krips, M., Cox, T. J., Matsushita, S., Mihos, J. C., & Pihlstrom, Y. 2009, *ApJ*, 695, 1537
- Jonsson, P. 2006, *MNRAS*, 372, 2
- Jonsson, P., Groves, B. A., & Cox, T. J. 2010, *MNRAS*, 186
- Juneau, S., Narayanan, D. T., Moustakas, J., Shirley, Y. L., Bussmann, R. S., Kennicutt, R. C., & Vanden Bout, P. A. 2009, *ApJ*, 707, 1217
- Kennicutt, Jr., R. C. 1998a, *ARA&A*, 36, 189
- . 1998b, *ApJ*, 498, 541
- Keres, D., Yun, M. S., & Young, J. S. 2003, *ApJ*, 582, 659
- Krumholz, M. R. & McKee, C. F. 2005, *ApJ*, 630, 250
- Krumholz, M. R., McKee, C. F., & Tumlinson, J. 2009a, *ApJ*, 693, 216
- . 2009b, *ApJ*, 699, 850
- Krumholz, M. R. & Thompson, T. A. 2007, *ApJ*, 669, 289
- Lee, H., Bettens, R. P. A., & Herbst, E. 1996, *A&AS*, 119, 111
- Leroy, A. K., Walter, F., Brinks, E., Bigiel, F., de Blok, W. J. G., Madore, B., & Thornley, M. D. 2008, *AJ*, 136, 2782
- McKee, C. F. & Ostriker, J. P. 1977, *ApJ*, 218, 148
- Mo, H. J., Mao, S., & White, S. D. M. 1998, *MNRAS*, 295, 319
- Narayanan, D., Cox, T. J., Hayward, C. C., Younger, J. D., & Hernquist, L. 2009a, *MNRAS*, 400, 1919
- Narayanan, D., Cox, T. J., & Hernquist, L. 2008a, *ApJ*, 681, L77
- Narayanan, D., Cox, T. J., Kelly, B., Davé, R., Hernquist, L., Di Matteo, T., Hopkins, P. F., Kulesa, C., Robertson, B., & Walker, C. K. 2008b, *ApJS*, 176, 331
- Narayanan, D., Cox, T. J., Shirley, Y., Davé, R., Hernquist, L., & Walker, C. K. 2008c, *ApJ*, 684, 996
- Narayanan, D., Dey, A., Hayward, C., Cox, T. J., Bussmann, R. S., Brodwin, M., Jonsson, P., Hopkins, P., Groves, B., Younger, J. D., & Hernquist, L. 2009b, *MNRAS* accepted: arXiv/0910.2234
- Narayanan, D., Groppi, C. E., Kulesa, C. A., & Walker, C. K. 2005, *ApJ*, 630, 269
- Narayanan, D., Hayward, C. C., Cox, T. J., Hernquist, L., Jonsson, P., Younger, J. D., & Groves, B. 2010, *MNRAS*, 401, 1613
- Narayanan, D., Kulesa, C. A., Boss, A., & Walker, C. K. 2006, *ApJ*, 647, 1426
- Narayanan, D. et al. 2008d, *ApJS*, 176, 331
- Noeske, K. G. et al. 2007a, *ApJ*, 660, L47
- . 2007b, *ApJ*, 660, L43
- Papadopoulos, P. P. & Ivison, R. J. 2002, *ApJ*, 564, L9
- Rosolowsky, E. 2005, *PASP*, 117, 1403
- . 2007, *ApJ*, 654, 240
- Sanders, D. B., Scoville, N. Z., & Soifer, B. T. 1991, *ApJ*, 370, 158
- Schaye, J. & Dalla Vecchia, C. 2008, *MNRAS*, 383, 1210
- Schmidt, M. 1959, *ApJ*, 129, 243
- Schöier, F. L., van der Tak, F. F. S., van Dishoeck, E. F., & Black, J. H. 2005, *A&A*, 432, 369
- Silk, J. 1997, *ApJ*, 481, 703
- Solomon, P. M., Rivolo, A. R., Barrett, J., & Yahil, A. 1987, *ApJ*, 319, 730
- Springel, V. 2000, *MNRAS*, 312, 859
- . 2005, *MNRAS*, 364, 1105
- Springel, V., Di Matteo, T., & Hernquist, L. 2005, *MNRAS*, 361, 776
- Springel, V. & Hernquist, L. 2003, *MNRAS*, 339, 289
- Tacconi, L. J. et al. 2010, *Nature*, 463, 781
- Tan, J. C. 2000, *ApJ*, 536, 173
- van Zadelhoff, G., Dullemond, C. P., van der Tak, F. F. S., Yates, J. A., Doty, S. D., Ossenkopf, V., Hogerheijde, M. R., Juvela, M., Wiesemeyer, H., & Schöier, F. L. 2002, *A&A*, 395, 373
- Walker, C. K., Adams, F. C., & Lada, C. J. 1990, *ApJ*, 349, 515
- Weiß, A., Downes, D., Walter, F., & Henkel, C. 2007, in *Astronomical Society of the Pacific Conference Series*, Vol. 375, *From Z-Machines to ALMA: (Sub)Millimeter Spectroscopy of Galaxies*, ed. A. J. Baker, J. Glenn, A. I. Harris, J. G. Mangum, & M. S. Yun, 25–+
- Wu, J., Evans, N., Shirley, Y., & Knez, C. 2010, *ArXiv e-prints*
- Wu, J., Evans, II, N. J., Gao, Y., Solomon, P. M., Shirley, Y. L., & Vanden Bout, P. A. 2005, *ApJ*, 635, L173
- Yao, L., Seaquist, E. R., Kuno, N., & Dunne, L. 2003, *ApJ*, 588, 771

